region has to be developed. This is expected to lead to somewhat different values for the additional intensity component I_z but will not change the general effect of this component on the SAXS curves.

Acknowledgment. I am indebted to Dr. A. R. Khokhlov for useful discussions.

References and Notes

(1) Ruland, W. *J. Appl. Crystallogr.* **1971**, *4*, 70.
(2) Vonk, C. G. *J. Appl. Crystallogr.* **1973**, *6*, 81.
(3) Todo, A.; Hashimoto, T.; Kawai, H. *J. Appl. Crystallogr.* **1978**, *11*, 558.
(4) Koberstein, J. T.; Morra, B.; Stein, R. S. *J. Appl. Crystallogr.* **1980**, *13*, 34.
(5) Roe, R.-J.; Fishkis, M.; Chang, J. C. *Macromolecules* **1980**, *14*, 1091.
(6) Siemann, U.; Ruland, W. *Colloid Polym. Sci.* **1982**, *260*, 999.
(7) Zin, W.-C.; Roe, R.-J. *Macromolecules* **1984**, *17*, 183.
(8) Annighöfer, F.; Gronski, W. *Makromol. Chem.* **1984**, *185*, 2213.
(9) Helfand, E.; Tagami, Y. *Polym. Lett.* **1971**, *9*, 741.
(10) Helfand, E.; Tagami, Y. *J. Chem. Phys.* **1972**, *56*, 3592.
(11) Semenov, A. N. *Zh. Eksp. Teor. Fiz.* **1985**, *88*, 1242.
(12) See, e.g.: Guinier, A. *Théorie et Technique de la Radiocristallographie*, 3rd ed.; Dunod: Paris, Chapter 13.6.
(13) Hermans, J. J. *Recl. Trav. Chim. Pays-Bas* **1944**, *63*, 5.
(14) Hadziioannou, G.; Mathis, A.; Skoulios, A. *Colloid Polym. Sci.* **1979**, *257*, 15.
(15) Hadziioannou, G.; Skoulios, A. *Macromolecules* **1982**, *15*, 258.
(16) Ruland, W. *Colloid Polym. Sci.* **1977**, *255*, 833.
(17) Ruland, W.; Tompa, H. *Acta Crystallogr., Sect. A: Cryst. Phys., Diffr., Theor. Gen. Crystallogr.* **1968**, *A24*, 93.

Light Scattering Characterization of an Alternating Copolymer of Ethylene and Tetrafluoroethylene. 1. Static and Dynamic Properties

Benjamin Chu* and Chi Wu

Chemistry Department, State University of New York at Stony Brook, Long Island, New York 11794. *Received April 17, 1986*

ABSTRACT: Laser light scattering, including the angular dependence of the absolute integrated scattered intensity and its spectral distribution, has been used successfully to characterize, for the first time, an alternating copolymer of ethylene and tetrafluoroethylene, $-(CH_2CH_2CF_2CF_2)_x-$, in diisobutyl adipate at 240 °C. In order to carry out experiments at high temperatures, we developed a new filtration apparatus and a new light scattering spectrometer capable of refractive index increment measurements. The results show that over the molecular weight range 5×10^5 to 1.2×10^6, our copolymer samples obey the scaling relations $\langle R_g^2 \rangle_z^{1/2} = 1.68 \times 10^{-1} M_w^{0.60}$ and $D_0° = 3.35 \times 10^{-4} M_w^{-0.60}$, with $\langle R_g^2 \rangle_z^{1/2}$, M_w, and $D_0°$ being the z-average root-mean-square radius of gyration (Å), the weight-average molecular weight, and the translational diffusion coefficient at infinite dilution (cm^2/s), respectively. Furthermore, the variance ($\mu_2/\bar{\Gamma}^2$) of the photoelectron count time correlation function shows a small value (~0.1), suggesting surprisingly narrow molecualr weight distributions for our copolymer samples.

I. Introduction

Laser light scattering (LLS) has been used to characterize a variety of polymers, including poly(1,4-phenylene terephthalamide) (PPTA)[1-5] and polyethylenes (PE).[6,7] The advantages of LLS are numerous. It is noninvasive. It has a wide dynamic range covering sizes from tens of angstroms to microns. The technique also permits determination of polydispersity in terms of molecular weight distributions, especially for unimodal functions of arbitrary shapes, without an a priori assumption on the form of the distribution function. In particular, LLS has been effective in characterizing polymer solutions at high temperatures,[6,7] e.g., at more than 200 °C for poly(dichlorophosphazene) in hexachlorotriphosphazene[8]), and polyelectrolytes (PPTA) in concentrated sulfuric acid, with and without added salt.[1-5] Thus, a natural extension and challenge in the application of LLS to polymer solution characterization is to examine static and dynamic properties of fluorocarbon polymers that defy characterization, simply because they are essentially insoluble in any ordinary solvents. Although our ultimate aim is to characterize poly(tetrafluoroethylene), $-(CF_2CF_2)_x-$, commercially known as Teflon (a registered trademark of Du Pont), we have to approach the characterization of poly(tetrafluoroethylene) (PTFE) slightly differently in view of the structural complexities associated with the solvent and plan to report our findings on PTFE later. In this (1) and a subsequent article (2), we report details of the characterization of a Teflon copolymer, an alternating copolymer of ethylene and tetrafluoroethylene (PETFE), $-(CF_2CF_2CH_2CH_2)_y-$. An outline of our procedures has already appeared in a preliminary publication.[9] Our report on the PETFE characterization can be divided into two parts. In this article (1), we shall be concerned with experiments on static and dynamic properties of PETFE in diisobutyl adipate at 240 °C, including a description of our new high-temperature light scattering spectrometer, adaptation for use as a high-temperature differential refractometer, and the development of a new high-temperature filtration apparatus for polymer solution clarification. In the subsequent article (2), we shall consider the determination of the molecular weight distribution (MWD) of PETFE from precise time correlation function measurements using experimentally determined scaling relations between the translational diffusion coefficient and the molecular weight and three different algorithms for the Laplace inversion. We report the details of our analysis in a separate article (2) because MWD can be determined only by means of LLS. At the present time, there is no other known technique that can provide an absolute determination of MWD of PETFE.

II. Experimental Methods

1. Materials. Diisobutyl adipate was obtained from Hatco Industries and was purified by passage through a column of activated silica gel to remove acidic and basic impurities. The resulting material was 99.5% pure by vapor phase chromatography. The polymers (courtesy of W. Buck, Polymer Products

0024-9297/87/2220-0093$01.50/0

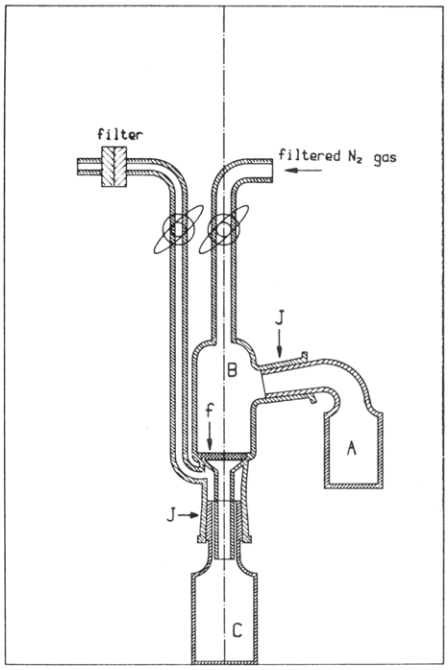

Figure 1. High-temperature dissolution/filtration apparatus. The entire apparatus can be placed in a high-temperature oven controlled at 250 ±2 °C. (A) Solution vessel, where we can introduce known weights of the dried polymer (PETFE) and the solvent (diisobutyl adipate) as well as a small glass-enclosed magnetic stirrer. (B) Filter, connected with A and C by means of clear seal glass joints (J) (14/20, Wheaton Scientific). f is a fine-grade sintered glass filter. (C) Cylindrical light scattering cell of 27-mm o.d. with a clear seal glass joint.

Department, Du Pont Experimental Station, Wilmington, DE) were commercial samples of Tefzel PETFE, manufactured by E. I. du Pont de Nemours and Co., and were used as received.

2. Preparation of Solutions. Solutions at different concentrations were prepared individually by dissolving known weights of the dried PETFE in diisobutyl adipate at 250 ± 2 °C.

A special dissolution/filtration apparatus was designed for this purpose. Such an apparatus constitutes a key element toward the success of our experiments. Furthermore, it should be useful for all high-temperature polymer solution clarifications. Therefore, we describe the apparatus, as shown in Figure 1, in some detail.

Known weights of PETFE and filtered diisobutyl adipate, as well as a small glass-enclosed magnetic stirrer, were placed in A at room temperature. The solution vessel (A) was connected to the precleaned filter (B). After degassing and introduction of nitrogen, both stopcocks were closed. PETFE was dissolved in diisobutyl adipate at 250 °C under constant stirring. It took about 1 h to dissolve the polymer completely. In order to ensure complete dissolution and homogeneity, we usually stirred the polymer solution for another hour before filtration. As the polymer solution in A was open to B, which was "open" to C through a fine-grade sintered glass filter, the volumes of B and C were kept small in order to reduce the volume available to the solvent vapor phase. When the polymer solution in A was ready for filtration, the solution vessel was turned 180° by means of the clear seal glass joint (J) between A and B. Then the polymer solution could be transferred to B without exposure to air at 250 °C. We used a gentle 10-psi nitrogen pressure to force the polymer solution directly into the precleaned dust-free cylindrical light scattering cell (C). This simple dissolution/filtration apparatus permits polymer solution preparation and clarification at high temperatures under an inert atmosphere without exposure to the external environment. Dust-free polymer solutions could be prepared with a very high rate of success with this apparatus. Furthermore, as the PETFE alternating copolymer has so few known solvents, we cleaned the all-glass dissolution/filtration apparatus by pyrolysis (~500 °C). As a consequence, the same apparatus could be used repeatedly without degradation of performance.

3. Methods of Measurement. A new high-temperature light scattering spectrometer was constructed for the PETFE characterization. Figure 2 shows the schematic top and side views of the essential features of the spectrometer, including the high-temperature thermostat and the detection optics.

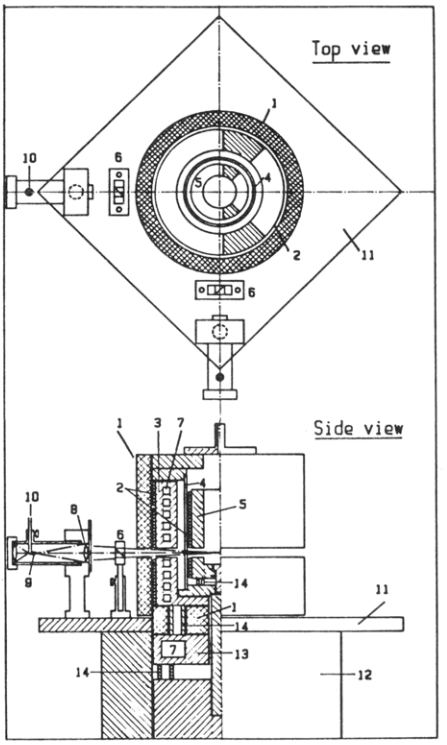

Figure 2. Schematic top and side views of the high-temperature thermostat and detection system of the light scattering spectrometer: (1) silicon rubber insulation; (2) heating wires for the brass thermostats; (3) outer brass thermostat with fluid circulation facilities; (4) vacuum glass jacket for thermal isolation (the glass jacket is made of precision polished glass of 2.25-in. o.d. with Kovar seals at both ends and machine-centered to coincide with the center of rotation of the turntable (12) to 0.001 in.); (5) inner brass thermostat, which has a separate te mperature controller and thermometer and can accommodate light scattering cells up to 27-mm o.d.; (6) Glan–Thompson polarizers; (7) fluid circulation paths; (8) lens; (9) field aperture; (10) optical fiber bundle; (11) rotating plate for multiple detectors; (12) RT-200 Klinger rotary table with 0.01° step size; (13) cooling plate to isolate the outer thermostat from the rotary table; (14) stainless steel standoffs for thermal isolation.

The essential features of the thermostat are as follows. We used a thermally controllable plate (13) as a heat sink which isolates the rotary table (12) from the outer thermostat (3) by means of two sets of stainless steel standoffs (14). The outer brass thermostat (3) was isolated from the room with 0.5-in.-thick porous silicone rubber. This arrangement created an oven that could be maintained easily in the 200–230 °C range with temperature fluctuations of less than 0.2 °C. A glass (vacuum) jacket of 2.25-in. o.d. was used to isolate the inner thermostat from the oven. The main function for the vacuum jacket was to reduce the temperature gradient in the light scattering cell. The inner thermostat had a separate temperature controller and a miniature platinum resistance thermometer that could be connected through the vacuum jacket by means of ceramic feed throughs. Figure 3 shows a typical tracing of the temperatures monitored by the thermometer located on the inner thermostat. Short-term (20 min) control of ±0.005 °C and intermediate-term (60 min) control of ±0.01 °C could be achieved at 240 °C, even in the absence of a vacuum. In a typical experiment, temperature could be controlled to ≤±0.03 °C during the entire experiment period, lasting around 10 h. For polymer solutions at high temperatures, it was important to test whether any appreciable degradation had taken place. All preparations and measurements were usually completed within a 12-h period and could be reproduced. The polymer concentration was checked independently by weighing the solution and, after evaporation, the polymer. The polymer solution began to have a yellowish tint after 36 h, and measurements could be

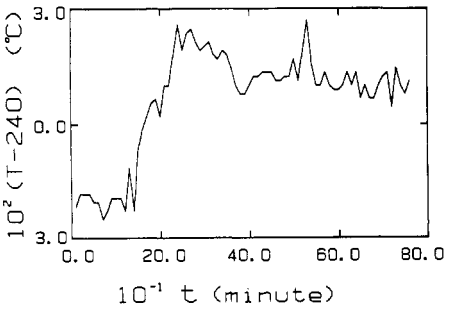

Figure 3. Typical temperature fluctuations of the inner thermostat at 240 °C. The large 20-min jump was due to a slight temperature readjustment. Short-term (20 min) temperature fluctuations were ~±0.005 °C. Intermediate-term (60 min) temperature fluctuations were ≲±0.01 °C. Long-term (10 h) temperature fluctuations were ≤±0.03 °C. The temperature gradient along the vertical axis (perpendicular to the scattering plane) was estimated to be ≲0.02 °C/cm in the absence of a vacuum.

reproduced within the first 36 h. One set of measurements was extended to ~100 h. We then observed a ~5% decrease in the characteristic decay times. However, as the light scattering cells were sealed only by the clear seal glass joint, we could not exclude a small amount of solvent evaporation.

The detection system consists of a 1 ft × 1 ft rotating platform (11) and various optical and mechanical components. Figure 2 shows the dual detection optics located 90° apart. Each detection "arm" has a lens (8) that transfers the scattering volume to the variable (e.g., ~0.7-mm diameter) field aperture (9) with a 2.5:1 ratio. The angular aperture is located in front of the lens (8), yielding a $\delta\theta$ of ~0.1°. The scattered light coming from well-defined scattering volume and angular aperture is transferred to the photomultiplier tube (EMI 9863) via an optical fiber bundle. It is important to have the appropriate optics *before* the optical fiber bundle, which acts only as a light pipe for the scattered light intensity. In this manner, the light scattering spectrometer could be reduced in size to a 1 ft × 1 ft platform, and simultaneous multiple-angle detection becomes feasible. With the platform, we can vary the angle between the two detection "arms" from about 10° to 160°. Simultaneous multiple-angle detection has the additional advantage of permitting time-dependent LLS studies of polymer solutions and gels. In our case, we could roughly shorten the measurement time by half using the dual-angle detection system. We used a Spectra-Physics Model 2020-03 argon ion laser operating nominally at ~150 mW and λ_0 = 488.0 nm.

Intensity measurements were accumulated automatically every 10° between the scattering angles θ of 30° and 120° for 10-s periods. No gating arrangement to exclude the effect of dust contributions was needed because the polymer solutions show little fluctuations in integrated scattered intensity which could be attributed to dust particles passing through the scattering volume.

Correlation function measurements were made with a 128-channel 4 × n correlator (Brookhaven Instruments, Model 2030). In the measured time correlation functions, the computed and measured base lines usually agreed to within 0.1%. The light scattering spectrometer was calibrated with benzene and NBS-705 polystyrene standard in cyclohexane.

III. Results and Discussion

1. Refractive Index and Refractive Index Increment Measurements. An absolute determination of the polymer molecular weight requires information on the refractive index increment (dn/dC) as well as the excess Rayleigh ratio (R_{vv}). A cylindrical light scattering cell was deformed to permit the exit laser beam to be refracted by the solution/air interface. The refraction could be measured and calibrated by using solvents of known refractive indices at room temperatures, as shown in Figure 4. Figure 5 shows a plot of refractive index of the solvent, diisobutyl adipate, as a function of temperature. We obtained n = 1.389 − 5.11 × 10^{-4}(T^* − 135 °C), with T^* expressed in °C. The refractive index of diisobutyl adipate

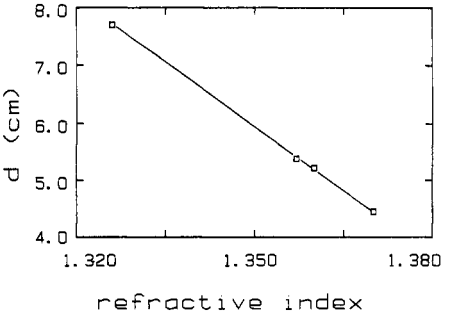

Figure 4. Calibration of a refractive index cell with different organic solvents at 25 °C and λ_0 = 488 nm. d denotes the laser beam displacement as measured by a micrometer. dd/dn = −7.385 × 10 cm with a resolution of ±0.001 mm.

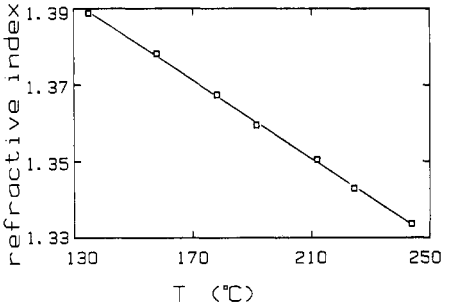

Figure 5. Refractive index of diisobutyl adipate as a function of temperature at λ_0 = 488 nm. dn/dT^* = −5.11 × 10^{-4} °C^{-1}. n = 1.389 − 5.11 × 10^{-4}(T^* − 135 °C), with T^* expressed in °C. The refractive index of diisobutyl adipate at 240 °C was estimated to be 1.334 at λ_0 = 488 nm.

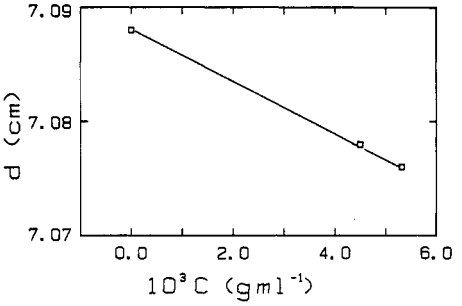

Figure 6. Plot of displacement d as a function of PETFE polymer concentration in diisobutyl adipate at 240 °C. dd/dc = −2.25 (cm mL)/g, corresponding to dn/dc = 0.031 mL/g at λ_0 = 488 nm.

at 240 °C was estimated to be 1.334. Figure 6 shows a plot of displacement d as a function of PETFE polymer concentration in diisobutyl adipate at 240 °C with $(\partial d/\partial C)_T$ = −2.25 (cm mL)/g. From our calibration, as shown in Figure 4, $(\partial d/\partial n)_T$ = −7.385 × 10 cm. Thus, we obtained the refractive index increment for PETFE in diisobutyl adipate: $(\partial d/\partial C)_T/(\partial d/\partial n)_T$ = 2.25/73.85 ≅ 0.031 mL/g at 240 °C using λ_0 = 488 nm. Although the calibration was performed at room temperature, the instrument showed negligible temperature effect over a 100 °C temperature change.

2. Light Scattering Intensity Measurements. The excess absolute integrated intensity of light scattered at a given angle from a dilute polymer solution has the form

$$\frac{HC}{R_{vv}(K)} \cong \frac{1}{M_w}\left(1 + \frac{K^2\langle R_g^2\rangle_z}{3}\right) + 2A_2C \qquad (1)$$

where $H = (4\pi^2n^2/N_A\lambda_0^4)(\partial n/\partial C)_T^2$, with λ ($\equiv\lambda_0/n$), A_2, $\langle R_g^2\rangle_z$, M_w, and K [$\equiv(4\pi/\lambda)\sin(\theta/2)$] being, respectively, the wavelength of light in the scattering medium, the second virial coefficient, the z-average mean-square radius

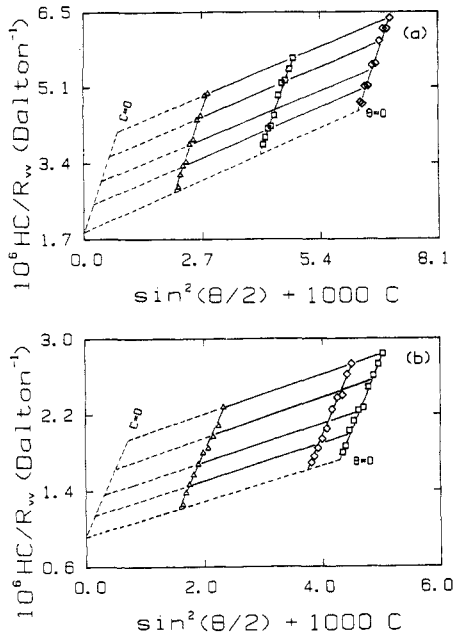

Figure 7. Zimm plots of PETFE in diisobutyl adipate at 240 °C using $\lambda_0 = 488$ nm. (a) $M_w = 5.4 \times 10^5$, $A_2 = 1.97 \times 10^{-4}$ g^{-1} mol^{-1} mL^2, $\langle R_g^2\rangle_z^{1/2} = 454$ Å: (Δ) $C = 2.09 \times 10^{-3}$ g/mL; (□) $C = 4.03 \times 10^{-3}$ g/mL; (◇) $C = 6.25 \times 10^{-3}$ g/mL. (b) $M_w = 1.16 \times 10^6$, $A_2 = 1.02 \times 10^{-4}$ g^{-1} mol^{-1} mL^2, $\langle R_g^2\rangle_z^{1/2} = 721$ Å: (Δ) $C = 1.57 \times 10^{-3}$ g/mL; (◇) $C = 3.75 \times 10^{-3}$ g/mL; (□) $C = 4.28 \times 10^{-3}$ g/mL.

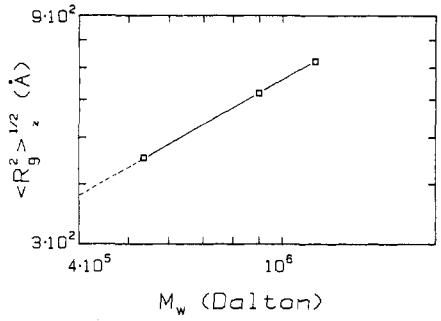

Figure 8. log–log plot of $\langle R_g^2\rangle_z^{1/2}$ vs. M_w for PETFE in diisobutyl adipate at 240 °C. Solid line denotes $\langle R_g^2\rangle_z^{1/2} = 0.168 \times M_w^{0.60}$, with R_g and M_w expressed in Å and daltons, respectively.

of gyration, the weight-average molecular weight, and the magnitude of the momentum transfer vector. The subscripts vv denote vertically polarized incident and scattered light. From a Zimm plot, as shown in Figure 7, we can determine the weight-average molecular weight, the second virial coefficient, and the z-average root-mean-square radius of gyration:

$$M_w: \quad \lim_{\substack{C\to0\\K\to0}} \frac{HC}{R_{vv}} = \frac{1}{M_w} \tag{2}$$

$$\langle R_g^2\rangle_z^{1/2}: \quad \lim_{C\to0} \frac{HC}{R_{vv}} = \frac{1}{M_w}\left(1 + \frac{K^2\langle R_g^2\rangle_z}{3}\right) \tag{3}$$

$$A_2: \quad \lim_{\theta\to0} \frac{HC}{R_{vv}} = \frac{1}{M_w} + 2A_2C \tag{4}$$

In a log–log plot of $\langle R_g^2\rangle_z^{1/2}$ vs. M_w, as shown in Figure 8, we obtained the scaling relation

$$\langle R_g^2\rangle_z^{1/2} = 1.68 \times 10^{-1} M_w^{0.60} \tag{5}$$

with R_g and M_w expressed in Å and daltons, respectively. Equation 5 suggested that the PETFE polymer molecules

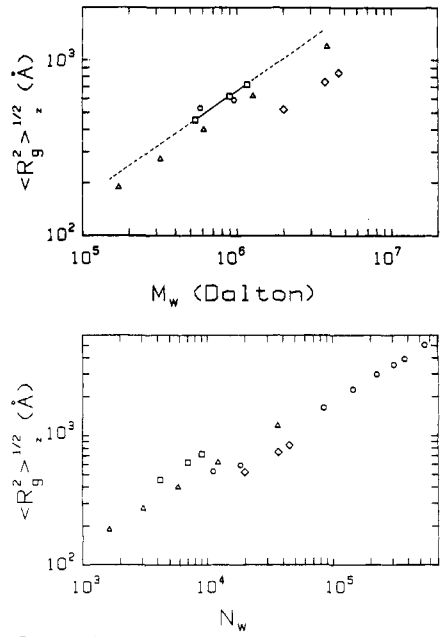

Figure 9. Comparison of radius of gyration of PETFE with those of other typical polymer coils: (a) R_g as a function of M_w; (b) R_g as a function of N_w ($\equiv M_w/M_0$, with M_0 being the segment unit consisting of 4-carbon atom backbones). Same solid line as in Figure 8. (Δ, ○) Polystyrene in benzene (ref 10 and 11, respectively); (◇) poly(methylene methacrylate) in methyl methacrylate (ref 12); (○) polyethylene in 1,2,4-trichlorobenzene (ref 7); (□) present work (R_g [Å] $= 1.68 \times 10^{-1} M^{0.60}$, with M expressed in daltons).

behave like coils, not wormlike chains. An absence of depolarized light scattering (or molecular anisotropy) further strengthened this supposition. Figure 9 shows a comparison of the radius of gyration of PETFE with those of other polymer coils. Its coil size did not exhibit any surprises; i.e., PETFE behaves more like other typical polymer coils in solution.

3. Light Scattering Line-Width Measurements.[6] The measured intensity–intensity time correlation function in the self-beating mode has the form

$$G^{(2)}(K,\tau) = A(1 + b|g^{(1)}(K,\tau)|^2) \tag{6}$$

where A is the background and b is a parameter depending on the detection optics. From eq 6, we can retrieve the normalized first-order electric field time correlation function $g^{(1)}(\tau)$, which for polydisperse polymer molecules in solution is related to the normalized characteristic line-width distribution function $G(\Gamma)$ by the Laplace integral equation:

$$g^{(1)}(K,\tau) = \int_0^\infty G(\Gamma) e^{-\Gamma(K)\tau}\, d\Gamma \tag{7}$$

In the present analysis we shall be concerned only with the method of cumulants, yielding an average line width $\bar{\Gamma}$ and the variance $\mu_2/\bar{\Gamma}^2$, with

$$\bar{\Gamma} = \int \Gamma G(\Gamma)\, d\Gamma \tag{8}$$

$$\mu_2 = \int (\Gamma - \bar{\Gamma})^2 G(\Gamma)\, d\Gamma \tag{9}$$

In the limit of low K ($KR_g < 1$), $\bar{\Gamma} = \bar{D}K^2$, where $\bar{D}$ is the z-average translational diffusion coefficient. Figure 10 shows typical plots of $\bar{\Gamma}/K^2$ vs. scattering angle θ for PETFE at different molecular weights and concentrations. By extrapolation of $\bar{\Gamma}/K^2$ to zero scattering angle, we determined the translational diffusion coefficient $D_0(C)$ [$\equiv \lim_{K\to0} \bar{\Gamma}/K^2$] at finite concentrations. From Figure 10,

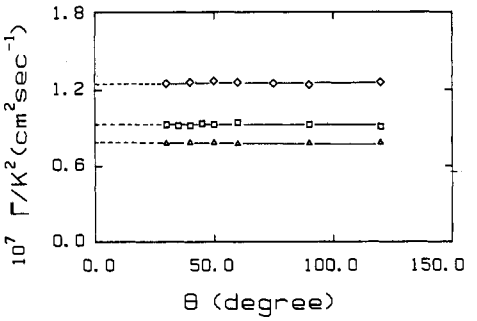

Figure 10. Typical plots of $\bar{\Gamma}/K^2$ vs. θ for PETFE in diisobutyl adipate at 240 °C: (□) $M_w = 9.0 \times 10^5$, $C = 3.50 \times 10^{-3}$ g/mL; (◇) $M_w = 5.4 \times 10^5$, $C = 4.03 \times 10^{-3}$ g/mL; (△) $M_w = 1.16 \times 10^6$, $C = 4.18 \times 10^{-3}$ g/mL.

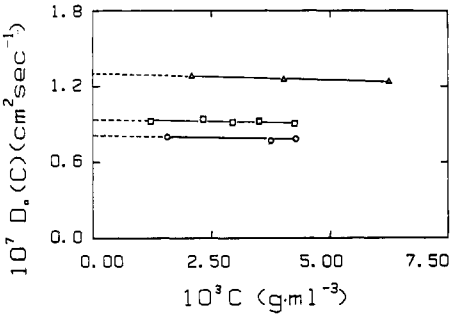

Figure 11. Plots of $D_0(C)$ as a function of concentration for PETFE in diisobutyl adipate at 240 °C: (□) $M_w = 9.0 \times 10^5$; (○) $M_w = 1.16 \times 19^6$; (△) $M_w = 5.4 \times 10^5$. As $k_d \sim 0$, $D_0° \sim D_0$.

we have also noted that the $\bar{\Gamma} = \bar{D}K^2$ relation is obeyed over the scattering angular range of our investigation for the PETFE polymers (up to $\sim 10^6$ dalton). Thus, in future characterizations of PETFE, this particular step can be ignored without appreciable error so long as $KR_g < 1$. In dilute solutions

$$D_0(C) = D_0°(1 + k_dC) \tag{10}$$

where $D_0°$ is the z-average translational diffusion coefficient at infinite dilution.

Figure 11 shows plots of $D_0(C)$ as a function of concentration for PETFE in diisobutyl adipate over a range of molecular weights at 240 °C. It is interesting to note that for PETFE in diisobutyl adipate at 240 °C, $k_d \simeq 0$ over the present molecular weight range of 5×10^5 to 1×10^6. Thus, by combining these two results, namely, $\bar{\Gamma} = \bar{D}K^2$ and $D_0(C) \simeq D_0°$, we can easily determine the molecular weight of the PETFE alternating copolymer in diisobutyl adipate at 240 °C by measuring only one characteristic line width at one scattering angle ($KR_g < 1$) and one finite concentration in the dilute solution region, provided that we know the scaling relation $D_0° = k_dM^{-\alpha_D}$. Figure 12 shows a log–log plot of $D_0°$ vs. M_w for PETFE in diisobutyl adipate at 240 °C. We obtained

$$D_0° = 3.35 \times 10^{-4}M_w^{-0.60} \tag{11}$$

with $D_0°$ and M_w expressed in cm^2/s and dalton, respectively. An exponent of 0.6 for α_D (eq 11) and α_R (eq 5) appears to suggest that the PETFE molecule is a polymer coil in a good solvent. Yet, we have noted that $k_d \sim 0$ and A_2 is positive but fairly small, suggesting that the solvent is not very good. A value of 0.60 for α_D could be expected to be too high since 0.60 is the upper limit for α_D in a polymer coil. Thus, it is likely that α_D is *less than* 0.60. It appears that the second virial coefficients, A_2 and k_d, could also exhibit a stronger temperature dependence than usual since PETFE is not soluble in diisobutyl adipate at even relatively high temperatures. A further investigation

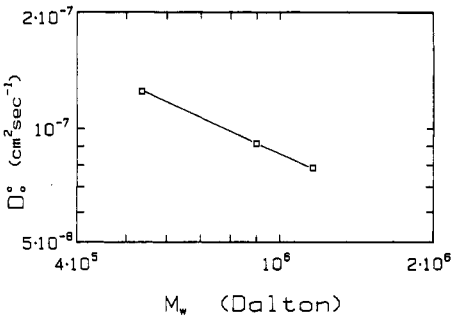

Figure 12. log–log plot of $D_0°$ vs. M_w for PETFE in diisobutyl adipate at 240 °C. Solid line denotes $D_0° = 3.35 \times 10^{-4}M_w^{-0.60}$, with $D_0°$ and M_w expressed in cm^2/s and daltons, respectively.

on the temperature dependence of the solvent quality and its relationship with the polymer melt temperature, as well as eq 11 covering a broader molecular weight range, is under way.

In Figure 9, we have noted that in a plot of R_g vs. N_w the sizes on a per-weight basis for PE and PETFE appear to be comparable while the same sizes on a per-segment basis are not the same, with R_g(per $-(CF_2CF_2CH_2CH_2)-$ segment) > R_g(per $-(CH_2CH_2CH_2CH_2)-$ segment). As the molecular weight range covered for PETFE (□) is very small (by a factor of 2) when compared with other studies, e.g., PS (△, ○; by a factor of >100), as shown in Figure 9, an α_D value of $\sim$0.6 must necessarily be taken to be qualitative in nature. The precaution in no way distracts from our finding that PETFE is surprisingly flexible.

It should be noted that copolymers of tetrafluoroethylene (TFE) and ethylene (E) have been studied by means of high-temperature, high-resolution FT NMR [^{1}H (90 MHz) and ^{19}F (84.68 MHz)],[13] infrared analysis,[14] and ESCA,[15] showing highly alternating structures with the equimolar copolymers alternating approximately 94% of the time. Thus, our analysis should remain valid for PETFE samples of comparable (equimolar) TFE/E compositions. Overall TFE/E composition variations can be taken into account by using experimentally measured refractive index increment.

Finally, in the cumulants method of data analysis, we obtained $\mu_2/\bar{\Gamma}^2 \sim 0.1$, suggesting a fairly narrow molecular weight distribution for our PETFE samples. The details are presented in paper 2.

IV. Conclusions

When the present PETFE samples are dissolved in diisobutyl adipate at 240 °C, polymer coils of fairly narrow molecular weight distribution are formed. The coil dimension appears to behave normally like those of other typical polymers such as polystyrene and poly(methyl methacrylate). Within the molecular weight range of our investigation, PETFE becomes an easy polymer to characterize since $k_d \sim 0$ and $\bar{D} = \bar{\Gamma}/K^2$ over typical accessible scattering angles (θ = 30–90°). Thus, with the relation $D_0°$ (cm^2/s) $= 3.35 \times 10^{-4}M_w^{-0.60}$, we can determine the molecular weight of PETFE using only one line-width measurement at a fixed scattering angle and at one finite concentration in the dilute solution regime by means of photon correlation spectroscopy. Furthermore, the cumulant method of data analysis is easily applicable for PETFE with such narrow molecular weight distributions. If we were interested only in the width of the MWD, the variance $\mu_2/\bar{\Gamma}^2$ ($\sim$0.1) is a clear indicator of polymer molecular polydispersity.

Acknowledgment. We gratefully acknowledge support of this work by the National Science Foundation, Polymers

Program (Grant DMR 8314193), and the U.S. Army Research Office (Contracts DAAG2985K0067 and DAAG2984G0080). B.C. thanks W. Buck for providing the PETFE polymers.

Registry No. (TFE)(E) (copolymer), 25038-71-5.

References and Notes

(1) Chu, B.; Ying, Q.; Wu, C.; Ford, J. R.; Dhadwal, H. S.; Qian, R.; Bao, J.; Zhang, J.; Xi, C. *Polym. Commun.* **1984**, *25*, 211.
(2) Ying, Q.; Chu, B. *Makromol. Chem., Rapid Commun.* **1984**, *5*, 785.
(3) Chu, B.; Wu, C.; Ford, J. R. *J. Colloid Interface Sci.* **1985**, *105*, 473.
(4) Ying, Q.; Chu, B.; Qian, R.; Bao, J.; Zhang, J.; Xu, C. *Polymer* **1985**, *26*, 1401.
(5) Chu, B.; Ying, Q.; Wu, C.; Ford, J. R.; Dhadwal, H. D. *Polymer* **1985**, *26*, 1408.
(6) Pope, J. W.; Chu, B. *Macromolecules* **1984**, *17*, 2633.
(7) Chu, B.; Onclin, M.; Ford, J. R. *J. Phys. Chem.* **1984**, *88*, 6566.
(8) For example, see: Chu, B.; Fytas, G.; Zalczer, G.; Lee, D. C.; Hagnauer, G. L. "Application of Light Scattering Spectroscopy to Polymerization Processes", invited presentation at the Symposium on Applications of Spectroscopy to Problems in Polymer Engineering and Science, 90th National Meeting of the American Institute of Chemical Engineers, Houston, TX, 1981.
(9) Chu, B.; Wu, C. *Macromolecules* **1986**, *19*, 1285.
(10) Adam, M.; Delsanti, M. *Macromolecules* **1977**, *10*, 1229.
(11) Miyaki, Y.; Einaga, Y.; Fujita, H. *Macromolecules* **1978**, *11*, 1180.
(12) Chu, B.; Lee, D.-C. *Macromolecules* **1984**, *17*, 926.
(13) English, A. D.; Garza, O. T. *Macromolecules* **1978**, *12*, 351.
(14) Modena, M.; Garbuglio, C.; Ragazzini, M. *J. Polym. Sci., Part B* **1972**, *10*, 153.
(15) Clark, D. T.; Feast, W. J.; Ritchie, I.; Musgrave, W. K. R. *J. Polym. Sci.* **1974**, *12*, 1049.

Light Scattering Characterization of an Alternating Copolymer of Ethylene and Tetrafluoroethylene. 2. Molecular Weight Distributions

Chi Wu,[†] Warren Buck,[‡] and Benjamin Chu*[†§]

Chemistry Department, State University of New York at Stony Brook, Long Island, New York 11794, Polymer Products Department, Experimental Station, E. I. du Pont de Nemours and Co., Inc., Wilmington, Delaware 19898, and Department of Materials Science and Engineering, State University of New York at Stony Brook, Long Island, New York 11794. *Received April 17, 1986*

ABSTRACT: By combining static and dynamic properties (M_w, A_2, k_d, R_g, and $D_0°$) of an alternating copolymer of ethylene and tetrafluoroethylene, $-(CF_2CF_2CH_2CH_2)_x-$, in diisobutyl adipate at 240 °C with a detailed analysis of the intensity–intensity time correlation function, we have been able to determine, for the first time, the molecular weight distribution (MWD) of an alternating copolymer of ethylene and tetrafluoroethylene (PETFE). A variety of Laplace inversion techniques, including multiexponential singular value decomposition (MSVD), a method of regularization (RILIE), and CONTIN, was used to obtain an estimate of the normalized characteristic line-width distribution function $G(\Gamma)$. The nonintrusive laser light scattering technique permits us to determine the molecular weight as well as the MWD of PETFE based on sound physical principles. Furthermore, in view of the simple $\Gamma = DK^2$ (with Γ, D, and K being the characteristic line width, the translational diffusion coefficient, and the magnitude of the momentum transfer vector, respectively) dependence and the second virial coefficient of diffusion, $k_d \sim 0$, the Laplace inversion used in the data analysis can be greatly simplified for determination of molecular weight and polydispersity of PETFE in diisobutyl adipate at 240 °C.

I. Introduction

In the previous paper (1), we characterized the solution properties of an alternating copolymer of ethylene (E) and tetrafluoroethylene (TFE), $-(CF_2CF_2CH_2CH_2)_x-$, denoted PETFE, in diisobutyl adipate at 240 °C, using laser light scattering intensity and line-width measurements. From light scattering intensity measurements, we obtained $\langle R_g^2\rangle_z^{1/2} = 1.68 \times 10^{-1} M_w^{0.60}$, with the z-average root-mean-square radius of gyration R_g [$\equiv\langle R_g^2\rangle_z^{1/2}$] and the weight-average molecular weight M_w expressed in units of Å and daltons, respectively. In combination with light scattering line-width measurements, we obtained $D_0° = 3.35 \times 10^{-4} M_w^{-0.60}$, with the translational diffusion coefficient at infinite dilution expressed in units of $cm^2\ s^{-1}$. In the present paper, the main steps are to obtain estimates of the normalized characteristic line-width distribution function $G(\Gamma)$ from the measured intensity–intensity time correlation function and to transform $G(\Gamma)$ to the molecular weight distribution (MWD) by means of the experimentally determined scaling relation $D_0° = k_D M^{-0.60}$. The main obstacle in the procedure is related to the relatively new method of data analysis: Laplace inversion of the electric field time correlation function:

$$g^{(1)}(K,\tau) = \int_0^\infty G(K,\Gamma) e^{-\Gamma(K)\tau}\, d\Gamma \qquad (1)$$

Although Laplace inversion is a difficult ill-posed problem because of the bandwidth limitation of our instrument and the noise in $g^{(1)}(K,\tau)$, there exists a variety of approaches (in particular, the method of regularization) permitting us to obtain approximate forms of $G(\Gamma)$ based on sound mathematical principles. Furthermore, several algorithms have undergone extensive tests using simulated data as well as actual experiments and have been applied to a variety of studies.[1,2] In an earlier laser light scattering study on the MWD of linear polyethylene,[3] we used the approach first developed by McWhirter and Pike,[4,5] while

[†] Chemistry Department, State University of New York at Stony Brook.
[‡] Polymer Products Department, E. I. du Pont de Nemours and Co.
[§] Department of Materials Science and Engineering, State University of New York at Stony Brook.

0024-9297/87/2220-0098$01.50/0